HHS Public Access

Author manuscript

Biol Psychiatry. Author manuscript; available in PMC 2021 November 15.

Published in final edited form as:

Biol Psychiatry. 2020 November 15; 88(10): 797–808. doi:10.1016/j.biopsych.2020.04.023.

Activation of Astrocytes in the Dorsomedial Striatum Facilitates Transition from Habitual to Goal-Directed Reward-Seeking Behavior

Seungwoo Kang[1,5], **Sa-Ik Hong**[1,5], **Jeyeon Lee**[2,3], **Lee Peyton**[1], **Matthew Baker**[1], **Sun Choi**[1], **Hyunjung Kim**[1], **Su-Youne Chang**[2], **Doo-Sup Choi**[1,4,*]

[1]Department of Molecular Pharmacology and Experimental Therapeutics, Mayo Clinic College of Medicine, Rochester, MN

[2]Department of Neurologic Surgery, Mayo Clinic College of Medicine, Rochester, MN

[3]Department of Radiology, Mayo Clinic College of Medicine, Rochester, MN

[4]Department of Psychiatry and Psychology, Mayo Clinic College of Medicine, Rochester, MN

[5]These authors contributed to this article equally

Abstract

BACKGROUND: Habitual reward-seeking behavior is a hallmark of addictive behavior. The role of dorsomedial striatum (DMS) in regulating goal-directed reward-seeking behavior has been long appreciated. However, it remains unclear how the astrocytic activities in the DMS differentially impact the behavioral shift.

METHODS: To investigate the astrocytic activity-driven neuronal synaptic events and behavioral consequences, we chemogenetically activated astrocytes in the DMS using GFAP promoter-driven expression of hM3Dq, the excitatory designer receptors exclusively activated by designer drugs (DREADDs). First, we confirmed the chemogenetically induced cellular activity in the DMS astrocytes using calcium imaging. Then, we recorded electrophysiological changes in the synaptic activity of the two types of medium spiny neurons (MSNs), direct and indirect pathway MSNs (dMSNs and iMSNs). To evaluate the behavioral consequences, we trained mice in nose-poke operant chambers that developed either habitual or goal-directed reward-seeking behaviors.

RESULTS: The activation of DMS astrocytes reduced the frequency of spontaneous excitatory postsynaptic currents (sEPSCs) in the dMSNs, whereas it increased the amplitude of the sEPSCs and decreased the frequency of spontaneous inhibitory postsynaptic currents (sIPSCs) in the iMSNs. Interestingly, astrocyte-induced DMS neuronal activities are regulated by adenosine metabolism, receptor signaling, and transport. Importantly, mice lacking an astrocytic adenosine

*Correspondence and request for materials should be addressed to Doo-Sup Choi, Ph.D., Department of Molecular Pharmacology and Experimental Therapeutics, Mayo Clinic College of Medicine, 200 First Street SW, Rochester, Minnesota 55905, USA or Department of Psychiatry and Psychology, Mayo Clinic College of Medicine, Rochester, Minnesota, 55905, USA, Phone: (507) 284-5602 Fax: (507) 284-1767 choids@mayo.edu.

transporter, ENT1 (equilibrative nucleoside transporter 1, Slc29a1) show no transition from habitual to goal-directed reward-seeking behaviors upon astrocyte activation, while restoring ENT1 expression in the DMS facilitated this transition.

CONCLUSIONS: Our findings reveal that DMS astrocyte activation differentially regulates the MSNs' activity and facilitates shifting from habitual to goal-directed reward-seeking behavior.

Keywords

astrocyte; habitual; goal-directed; reward-seeking; dorsomedial striatum; adenosine

INTRODUCTION

Maladaptive shifts in goal-directed to habitual actions may lead to severe psychopathologies such as obsessive-compulsive disorder, impulsivity, and addiction (1). Indeed, persistent habitual reward-seeking, characterized by insensitivity to reversal of action-outcome contingency, even after reward devaluation, is a common feature of addiction (1–3). However, neural mechanisms underlying these reward-seeking behavioral patterns are still not fully understood.

The dorsal striatum (DS) has a critical role in shaping goal-directed and habitual actions, which are the main determinants for the reward-dependent decision-making process (1). Specifically, the medial part of the DS (DMS) contains neuronal populations responsible for goal-directed behavior. DMS neurons are mainly composed of D1R-containing direct- and D2R/A2AR-containing indirect-pathway medium spiny neurons (dMSNs and iMSNs). Interestingly, these dMSNs and iMSNs have been frequently shown to diverse responses even by the same stimulus because of the different neuronal properties such as distinguishable circuits of excitatory/inhibitory neurotransmissions from upstream brain regions (4–7) and selective expression of GPCRs in the dMSNs and iMSNs (8–10). Since lesions or inactivation of the DMS prevents goal-directed behavior and promotes habitual behavior (11), the combinational modulation of those neurons has been implicated in the shaping of reward-seeking behavioral patterns. Indeed, shifts in neuronal activity in the DMS corresponds to transition between goal-directed and habitual actions (12–14).

Recently, in addition to well-known neuro-supportive roles, astrocytes are emerging as a key determinant of neuronal synaptic function and consequent behavioral changes (15–21). Astrocyte activity is attributed to behavioral consequences through the release of various gliotransmitters including ATP, adenosine, D-serine, and glutamate (18, 19, 22–25). Thus, the homeostatic role of astrocytes has been examined through the disruption of its molecular events to identify astrocyte regulation in the pathological neuronal activities and behaviors (26–28). However, it remains unknown how temporal astrocyte activity regulates the synaptic and circuit functions in the DMS underlying the transition between goal-directed and habitual reward-seeking.

In the present study, using designer receptors exclusively activated by designer drugs (DREADDs), we were able to activate astrocytes temporospatially in the DMS. Using chemogenetic, optogenetic, electrophysiological, and behavioral approaches, we revealed a

novel role of astrocytes in the regulation of dorsomedial neuronal activities in a purine-dependent manner and subsequent behavioral shift in reward-seeking behavior patterns.

METHODS AND MATERIALS

Animals

All experimental procedures were approved by the Mayo Clinic Institutional Animal Care and Use Committee and performed in accordance with NIH guidelines. Adenosine A2A receptor (A2AR: Adora2A, MMRRC:031168-UCD)-Cre mice were provided by Dr. Jiang-Fan Chen at Wenzhou Medical University. Aldehyde dehydrogenase 1 family, member L1 (ALDH1L1)-Cre (Stock #023748), Dopamine D2 receptor (D2R: DRD2)-eGFP (stock #030255), Dopamine D1 receptor (D1R: DRD1)-tdTomato (stock #016204) and C57BL/6J mice were purchased from Jackson Laboratory (Bar Harbor, ME). The ENT1 KO mice were generated as described (27). Mice were housed in standard Plexiglas cages and the colony room was maintained at a constant temperature (24 ± 1°C) and humidity (60 ± 2%) with a 12 h light/dark cycle (lights on at 07:00 A.M.). We used 8- to 10-wk-old male mice for all experiments.

Stereotaxic surgery for virus injection and behavior experiments

Stereotaxic surgery was performed to infuse virus into the DMS (AP +0.6 mm, ML +1.35 mm, DV −2.35 mm from bregma). *1) Instrumental behavior training*. Mice were trained on a random interval or a random ratio context to develop habitual and goal-directed seeking, respectively. The detailed training procedures are provided in Supplemental Methods and Materials. *2) Extinction test*. On the devalued day, mice were given 1h of *ad libitum* access to the outcome (sucrose) previously earned by nose poke (for devaluation), or food pellet and then underwent serial non-reinforced test sessions in each training context. The order of context exposure during testing was the same as training exposure with the order of valuation day counterbalanced across mice. Tests in each context were 10 min in duration. The devaluation index were calculated based on nose-poking (NP) rate: $(\text{NP rate}_{\text{valued}} - \text{NP rate}_{\text{devalued}}) / (\text{NP rate}_{\text{valued}} + \text{NP rate}_{\text{devalued}})$ (29, 30).

Electrophysiology

The details in brain slice preparation, *ex vivo/in vivo* electrophysiology, and optogenetics are provided in Supplemental Methods and Materials. The dMSNs and iMSNs were identified with the expression of fluorescence including GFP and mCherry and electrophysiological properties (31, 32).

Drugs

We purchased common chemicals from Sigma Aldrich (St. Louis, MO, USA) except DPCPX, PSB12379, and NBTI (NBMPR) which were purchased from Tocris (Minneapolis, MN, USA).

Statistical analysis

All data represented as the mean ± S.E.M. and were analyzed by unpaired/paired two-tailed student's *t*-tests, one-way analysis of variance (ANOVA)/repeated measures one-way ANOVA followed by Tukey's or Bonferroni's multiple comparisons tests, and two-way ANOVA/repeated measures ANOVA followed by Tukey's or Bonferroni's multiple comparisons tests using Prism 8.0 (GraphPad Inc., San Diego, CA, USA). Statistical significance was set at $P < 0.05$. Detailed statistical data with exact P values are listed in the Table S1.

RESULTS

Selective Activation of Excitatory DREADDs Induces Calcium Signaling in the DMS Astrocytes.

Previous studies have demonstrated that endogenous Gq-GPCRs induce calcium influx in astrocytes (33–36), thereby promoting astrocyte-neuron interaction and results in behavioral changes (18, 21, 37–40). In order to induce astrocyte activity, we selectively expressed the Gq-coupled DREADDs in GFAP-expressing cells in the DMS by microinjection of adeno-associated virus serotype 5 (AAV5) containing a GFAP promoter-driven gene that encodes the modified M3-muscarinic receptor fused to mCherry (hM3Dq-mCherry) (Figure 1A–D). We confirmed that DREADDs are expressed in astrocyte cells by co-immuno-labeling anti-GFAP with mCherry expression (Figure 1B), while no co-localization was observed with the neuronal marker, anti-NeuN, or the microglial marker, anti-Iba1, antibodies in the DMS (Figure 1C,D).

We then examined calcium dynamics with the genetically encoded calcium-sensitive fluorescent proteins, GCaMP6s (41). We first measured the effects of chemogenetic activation in the astrocyte calcium events in the DMS using ALDH1L1 promoter-driven GCaMP6s expressing mice (Figure 1E,F). In *ex vivo* recordings, bath application of Compound 21 (C21, a DREADDs ligand, 10 μM) significantly triggered an intracellular Ca^{2+} increase in hM3Dq-expressing astrocytes in comparison to the recordings in which vehicle was applied to hM3Dq-expressing astrocytes or C21 was applied to non-hM3Dq expressing astrocytes [one-way ANOVA, $F(2,37)=27.00$, $P<0.05$; *post-hoc*: no-hM3Dq/C21 vs. hM3Dq/C21, $P<0.05$; hM3Dq/Veh vs. hM3Dq/C21, $P<0.05$, Figure 1G–I]. C21 application in the astrocytes without the expression of hM3Dq had no difference compared to vehicle treatment [no-hM3Dq/C21 vs. hM3Dq/Veh, NS (not significant), Figure 1I], indicating the changes in events were not due to the effects of C21 application itself. Importantly, systemic administration of C21 (1 mg/kg, *i.p.*) to free-moving mice also significantly increased calcium-indicating events in the DMS astrocytes as compared to those after saline injections (paired *t*-test; frequency: $t=6.27$, $P<0.05$, Figure 1J,K; total time: $t=3.78$, $P<0.05$, Figure 1J,L). Collectively, we confirmed the specific and selective expression as well as activation of hM3Dq in the DMS astrocytes.

Chemogenetic Activation of DMS Astrocytes Differentially Regulates the Spontaneous Synaptic Events in Direct and Indirect MSNs and GPe Neurons.

Based on previous observations (42–44), to determine the effects of astrocyte activation on the medium spiny neuron (MSN) subtypes that comprise >90% of all DMS neurons (Figure S1), we performed whole-cell recordings in the MSNs of mice expressing hM3Dq in the astrocytes of the DMS (Figure 2A,B). Since we targeted the neurons at a depth of more than 100 μm in the slice, the whole structure of both the recorded neurons and the surrounding astrocytes could be preserved. In the voltage-clamp whole-cell recordings, we found that C21 application resulted in decreased frequency of spontaneous excitatory postsynaptic currents (sEPSCs) in the direct-pathway MSNs (dMSNs, paired *t*-test, frequency: $t=3.49$, $P<0.05$; amplitude: $t=1.10$, NS, charge transfer: $t=1.12$, NS), while it increased the amplitude of sEPSCs in the indirect-pathway MSNs (iMSNs, paired *t*-test, frequency: $t=0.19$, NS; amplitude: $t=4.63$, $P<0.05$, charge transfer: $t=1.38$, NS). Importantly, the activation also induced a significant decrease in spontaneous inhibitory postsynaptic currents (sIPSCs) in the iMSNs (paired *t*-test, frequency: $t=4.45$, $P<0.05$; amplitude: $t=3.63$, $P<0.05$, charge transfer: $t=2.89$, $P<0.05$).

Next, we examined whether the astrocyte activation physiologically dampens the external globus pallidus (GPe), the main output of DMS iMSNs (45). We employed A2AR-Cre mice to examine the activity of iMSNs because D2-containing iMSNs in the DMS are mostly co-expressing A2AR (>99%, Figure 3A). We co-injected GFAP promoter-driven hM3Dq expressing and Cre-dependent channelrhodopsin(ChR2)-expressing AAV5 into the DMS of A2AR-Cre mice to measure the electrophysiological features in the GPe after the DMS astrocyte activation (Figure 3A,B). To confirm whether the neurons we recorded in the GPe were receiving a signal from DMS, we expressed ChR2 in the A2AR-expressing iMSNs in the DMS and recorded neuronal responses in the GPe (Figure 3A,B). Blue light stimulation in the DMS inhibited the spontaneous firing in the GPe (Figure 3C,D), verifying that the neurons measured in the GPe were receiving inhibitory signaling from the DMS iMSNs (45). Importantly, systemic application of C21 (1 mg/kg, *i.p.*) without light stimulation significantly reduced the spontaneous firing in the GPe of mice expressing astrocyte hM3Dq in the DMS compared to those without hM3Dq expression (unpaired *t*-test, $t=3.98$, $P<0.05$, Figure 3E,F). This indicates that the local astrocytic activation-induced changes in the neuronal events could alter the activity of the downstream circuit.

DMS Astrocyte Activation Abolishes Habitual Reward-Seeking Behaviors.

Based on our findings that astrocyte activation is sufficient to induce cell-type specific changes in activities of MSNs in the DMS and also on the previous studies demonstrating the contribution of the DMS toward reward and decision-making behaviors (11, 14, 44–47), we sought to test whether astrocyte activation can affect reward-seeking behaviors. We trained mice expressing hM3Dq in astrocytes of the DMS with an operant-conditioning method by random interval (RI) to establish habitual reward-seeking behavior (Figure 4A,B). In accordance with the training schedule, mice acquired nose-poking behavior through a fixed ratio 1 schedule (FR1) followed by 1 day of RI30 and 2 days of RI60, mice progressively chose the active hole compared to the inactive hole [two-way ANOVA, for group $F(1,26)=20.93$, $P<0.001$, Figure 4C] with reduced latency to magazine compared to

the first FR1 session [one-way ANOVA, for group $F(2,26)=4.17$, $P<0.05$, *post-hoc*: FR1 1st day vs. 3rd day $P<0.05$, Figure 4D].

To test the effect of astrocyte activation on the behavioral patterns of reward-seeking, C21 was administered 30 min before the extinction test, in which mice were tested in the same operant chambers for 10 min without the reward. C21 application (1 mg/kg, *i.p.*) did not induce any changes in nose-poking rates in valued states (paired *t*-test, $t=0.41$, NS, Figure 4E). In the devaluation test, which compares nose-poking between the valued and devalued condition, vehicle-treated mice did not show a decrease in nose-poking in the devalued condition, indicating a habitual behavior (paired *t*-test, $t=0.94$, NS, Figure 4F). This is consistent with previous studies showing that a RI schedule yields conditioned habitual reward-seeking behavior (1, 12, 13, 48). Interestingly, mice injected with C21 were markedly sensitive to outcome devaluation (paired *t*-test, $t=2.83$, $P<0.05$, Figure 4F), indicating that the activation of DMS astrocytes promoted goal-directed behavior. C21 application did not alter locomotor activity (paired *t*-test, distance traveled: $t=0.35$, NS; velocity: $t=0.63$, NS, Figure S2). When we trained the mice to develop goal-directed behaviors through a random ratio paradigm (Figure S3), the astrocyte activation in the DMS did not induce behavioral changes (paired *t*-test, $t=4.55$, $P<0.05$, Figure S3D), indicating DMS astrocyte activation specifically reduces habitual, but not goal-directed behaviors toward a conditioned reward.

Adenosine Signaling is Involved in DMS Astrocyte Activation-induced Neuronal activity and Habitual Reward-Seeking Behaviors.

Gliotransmitters, including glutamate, D-serine, ATP, and adenosine, have been shown to modulate neuronal synaptic transmission (17, 49–52). Our previous data showed that adenosine signaling in the MSNs of the DMS modulates reward-seeking behaviors (45, 46). Interestingly, direct bath application of adenosine *ex vivo* induces changes in synaptic events of dMSNs and iMSNs, which are similar to those induced by the astrocyte activation (paired *t*-test, in the dMSNs, frequency: $t=7.43$, $P<0.05$, amplitude: $t=0.84$, NS; in the iMSNs, frequency: $t=0.15$, NS, amplitude: $t=2.86$, $P<0.05$, Figure S4). Thus, to examine the role of adenosine signaling in the observed synaptic events, we first tested the pharmacological effects of inhibited adenosine signaling (Figure 5A–E, Figure S5). The pretreatment of a selective adenosine receptor A1R antagonist (DPCPX, 1 μM) abolished the astrocyte-induced reduction in the frequency of sIPSCs of the iMSNs [one-way ANOVA, for treatment $F(3,23)=9.48$, $P<0.05$, *post-hoc*: CON vs. DPCPX, $P<0.05$, Figure 5B–E]. Since extracellular adenosine levels are known to be regulated by both ectonucleotidases that metabolize ATP to adenosine and astrocyte adenosine transporters (46, 53, 54), we subsequently tested the roles of PSB12379, an inhibitor of an ectonucleotidase, CD73, and NBTI, an inhibitor of equilibrative nucleoside transporter 1 (ENT1, the astrocyte adenosine transporter), respectively. The pretreatment of PSB12379 (10 μM) significantly reduced the C21-induced changes in the sIPSCs of iMSNs (*post-hoc*: CON vs. PSB12379, $P<0.05$, Figure 5E) although it was not completely blocked (paired *t*-test, $t=2.48$, $P<0.05$, Figure 5D). The C21-induced changes in the sIPSCs were also reduced by NBTI (10 μM, *post-hoc*: CON vs. NBTI, $P<0.05$, Figure 5E). Interestingly, the C21-induced changes in sIPSC were

also reduced in the DMS of mice with the genetic deletion of ENT1 (ENT1 KO vs. ENT1 WT, Unpaired *t*-test, t=2.73, P<0.05, Figure 5F–H)(27).

Since the ablation of ENT1 inhibits the changes in synaptic events induced by the astrocyte activation in the DMS, we tested whether it also affects reward-seeking behaviors (Figure 6A–C). Indeed, during devaluation testing, the C21 application, even with a higher dose (3 mg/kg, *i.p.*), did not decrease nose-poking in the devalued condition, showing no significant devaluation effect in ENT1 KO mice (paired *t*-test, 1 mg/kg: t=1.17, NS; 3 mg/kg: t=0.74, NS, Figure 6C, Figure S6). Collectively, these pharmacological and genetic validations suggest that adenosine signaling is, at least partly, required in the astrocyte-induced DMS neuronal adaptation and the shifting of reward-seeking behaviors.

Other gliotransmitters also possibly alter the neuronal synaptic transmission induced by the astrocyte activation (55). Similar to our previous results showing no difference in the extracellular glutamate levels measured by microdialysis between ENT1 wild-type and KO in the dorsal striatum (46, 56), the systemic application of C21 in mice expressing astrocyte hM3Dq in the DMS did not change the homeostatic levels of glutamate (CON vs. C21, paired *t*-test, t=0.37, NS, Figure S7). This suggests that the neuronal adaptation and behavioral shifts are unlikely caused by the glutamate release from astrocytes.

Restoring of Astrocyte ENT1 Expression in the DMS Normalizes the Astrocyte-Induced Reward-Seeking Behaviors

Since the reward-seeking behavioral shift induced by the DMS astrocyte activation was not observed in the ENT1 KO mice (Figure 6A–C), we sought to determine if the restoring of ENT1 expression in the DMS reinstates the behaviors (Figure 6D–G). We injected a virus to express ENT1 in astrocytes utilizing the GFAP promoter (Figure 6D,E). ENT1 rescue in the DMS did not affect the expression of adenosine receptors in the DMS (Figure S8). During the devaluation test, the mice expressing astrocyte ENT1 became markedly sensitive to the outcome devaluation through decreased nose-poking after C21 application (paired *t*-test, 1 mg/kg: t=6.08, P<0.05; 3 mg/kg: t=6.20, P<0.05, Figure 6G). The C21-induced changes in reward-seeking behavioral patterns were significantly different from those of ENT1KO mice without ENT1 overexpression in the DMS [two-way ANOVA, for genotype F(1,45)=12.13, P<0.05, Figure 6H], indicating that ENT1 overexpression in the DMS of ENT1 KO mice abolished the astrocyte-driven habitual actions as observed in wild-type mice.

Taken together, our finding supports the hypothesis that the GPCR Gq-pathway driven increase in astrocyte calcium signaling of the DMS alters the microcircuits between astrocytes and neurons, leading to the shift in patterns of reward-seeking behaviors, at least partly, via adenosine signaling.

DISCUSSION

In the present study, we provide a novel aspect of the interaction between astrocytes and neurons in the DMS, which regulates habitual and goal-directed behaviors. This is, to the best of our knowledge, the first time showing that the activation of astrocytes abolishes habitual reward-seeking behavior and promotes a transition to goal-directed reward-seeking

behavior as summarized in Figure 7. For this study, we took advantage of a chemogenetic DREADDs approach that allows us to spatiotemporally activate the astrocytes in the DMS, which can mimic the GPCR-Gq pathway-driven activation of astrocytes. Our data showed that the behavioral shifts from habitual action to goal-directed behaviors were evoked by activating astrocytes but were blunted by pharmacological and genetic depletion of adenosine signaling. In addition, we provide evidence that DMS astrocytes could alter the neuronal activities in the downstream circuit, indicating the importance of local microcircuits in broad brain activities and behavioral consequences. Thus, this study reveals the direct role of astrocytes as determinants of neuronal activities and behavioral outcomes in reward-seeking.

Our data indicate that astrocytes in the DMS are functional components of the adenosinergic system. Consistent with the reports of other brain regions, the adenosinergic system is one of the key determinants of astrocytes regulating synaptic transmission through Ca^{2+} influx in the astrocytes, which induces subsequent calcium mobilization and the stimulation of gliotransmitter release (57, 58). The synaptic regulation observed in this study parallelly happens with the astrocyte calcium activity that stimulated the release of ATP/adenosine, which is acting as a gliotransmitter. Thus, it evokes the effects of the occupation of the neuronal adenosine receptors in the DMS synapses similar to what we observed in recent studies demonstrating pharmacological, optogenetic, and genetic modification of adenosine A2AR in the DMS has an important role in reward-seeking behaviors (45, 46). In addition, the ATP-derived adenosinergic system regulates synaptic transmission and plasticity through the metabolism in the extracellular area by the activities of ectonucleotidase, which can hydrolyze ATP to adenosine (16, 50). However, the direct release of adenosine by adenosine transporters has not been fully studied. Thus, the present results add to the accumulating evidence indicating that the adenosine transporter may have additional synaptic regulatory effects in the context of activated astrocytes. These transporters can expand the signaling range and regulate synapses distant from the homeostatic extracellular adenosine levels, which affects the neuronal activities slowly (59). Interestingly, whereas the pretreatment of ectonucleotidase inhibitor, which potentially prevents the metabolism of ATP to adenosine, reduces the astrocyte-activation induced changes in the GABAergic synaptic events mainly in post-synapses, the pretreatment of ENT1 inhibitor that blocks the transport of adenosine reduces mainly the events in pre-synapses. This raises the possibility that the purinergic signaling has been modulated by several layers in a spatially- and temporally-dependent manner and those layers have different characteristics according to what proximity they have in the connections with synapses. These complementary mechanisms of adenosine-driven astrocyte-neuron interaction reveal a complex neural network which is required for the fine regulation of reward-seeking behavior.

The selective signaling of astrocytes to specific synapses from distinct neuronal populations has been reported recently in basal ganglia circuits (4). The synapse specificity of astrocyte signaling is further supported by the present results, which show that adenosine derived from astrocytes distinctly regulates excitatory and inhibitory synaptic transmission in the DMS by activating specific adenosine receptors. Our findings indicate that while the astrocytic activation in the DMS induces the decrease in sEPSCs in the dMSNs, it induces the increase in sEPSCs and the decrease in sIPSCs (disinhibition) in the iMSNs that may simultaneously

drive the increased neuronal activities. Interestingly, astrocyte activation tremendously reduces the GABAergic signaling in the iMSNs but not in the dMSNs. Therefore, rather than triggering broad and non-specific effects, astrocytes exert their regulatory actions through selective interaction with specific synapses via the activation of the signaling pathways. In addition, since we show that the MSN-specific regulation by astrocytes yields critical behavioral consequences, further characterization of the pre- and post-synapses is also warranted to resolve the different mechanisms of modulation following activation of astrocytes in the DMS. For example, it would be intriguing to investigate whether the observed differences in MSNs' GABAergic signaling is from local interneurons or upstream brain regions (60, 61).

Besides adenosine, astrocytes are able to release different neuroactive substances. Indeed, other gliotransmitters, including glutamate and D-serine, are also identified as regulators of specific behaviors and synaptic transmission in brain areas (17, 19, 49–52). For example, several GPCRs and ion channels including μ-opioid receptors, CB1 receptors, and TWIK-1/TREK-1 heterodimers mediate astrocyte activation and glutamate release from astrocytes (4, 55, 62). However, our microdialysis data does not show the significant changes in the glutamate in the DMS after the activation of astrocytes, suggesting that the regulation of the gliotransmitter glutamate in astrocytes is not implicated in this context. Instead of the changes in the amount of extracellular glutamate and also potentially GABA, the observed changes in synaptic events seem to be involved in the modulation of the potential of the receptors in synapses. Thus, in our experimental paradigm, it is unlikely that other gliotransmitters might be the major determinant for the observed behavioral outcomes.

The cell-type specificity was demonstrated by showing that hM3Dq-mCherry was expressed in only GFAP-positive cells, but not in NeuN- or Iba-expressing cells. In the CNS, GFAP expression is commonly used to identify differentiated astrocytes. Although we cannot conclusively exclude the existence of GFAP-positive progenitor cells who produce neurons and oligodendrocytes throughout the CNS (63), the relatively fast responses in the neurons after activation of GFAP-positive cells suggest to us a rare possibility that the population of GFAP positive are progenitor cells. Thus, our data suggest that astrocytes are the major cells activated by DREADDs. In addition, although astrocytes are ubiquitous in the brain, region-specific characteristics have been previously reported (36). It would be interesting to further characterize the detailed role of astrocytes using the DREADDs with different promoters such as ALDH1L1 or mucrystallin (64).

Behavioral flexibility is the process of responding and adapting to associated stimuli appropriately, thereby inhibiting maladaptive actions (65). This action-outcome process that influences decision making and reward-seeking behaviors is associated with the combined activity of dMSNs and iMSNs in the DMS (12, 14). In our animal model, astrocyte activity in the DMS "during the extinction test" facilitates the transition from habitual action to a goal-directed behavioral state. Since many psychiatric disorders, including addiction, are normally accompanied with the formation of maladaptive habitual behavior, it is common for patients to be treated with exposure therapy which is designed to extinguish the developed habitual behavior (66). These findings may direct attention toward astrocyte activity as a potential component in therapeutic treatment that could facilitate extinction in

maladaptive habitual behavior. However, despite the role of astrocyte activity during the extinction process, the precise role of astrocytes in the development of habitual behaviors during repeated exposures to motivating stimuli is still unclear. The time- or stage-dependent astrocyte activation is necessary to determine the role of astrocytes during the development and extinction of reward-seeking patterns.

We manipulated the activity of DMS astrocytes in free-moving mice by utilizing a combination of AAV-driven overexpression of hM3Dq DREADDs in the DMS and systemic administration of DREADDs' ligand. Notably, we showed that C21 induces a significant increase in Ca^{2+} signaling in the DMS astrocytes of mice expressing hM3Dq in astrocytes, indicating that systemic administration of C21 activates the brain regional activities. In regard to DREADDs system *in vivo*, some recent studies discussed potential complications of utilizing chemogenetics, which include brain penetrance and off-target metabolite effects. For example, clozapine, a metabolite of DREADDs activator, mediates the effects on non-DREADDs receptors in the brain (67–69). Thus, in this study, we utilized compound 21 (C21) (11-(1-piperazinyl)-5H-dibenzo[b,e][1,4]diazepine) instead of CNO (clozapine-*N*-oxide), since C21 is a potent and selective agonist at both excitatory (hM3Dq) and inhibitory (hM4Di) DREADDs and has excellent bioavailability, pharmacokinetic properties, and brain penetrability. Particularly, C21 represents an alternative to CNO for *in vivo* studies where the metabolic conversion of CNO to clozapine is a concern (70). We employed the doses of C21 that are known not to affect animal behavior (68, 69). To avoid possible off-target effects of C21, we also validated the C21 effects in mice without DREADDs expression.

In summary, the characterization of the synaptic events and reward-seeking patterns according to the astrocyte activation in the DMS provides a possible signaling pathway that demonstrates how adenosine signaling alters the activities of the DMS and DMS-GPe circuit. Together, our findings provide a novel aspect of reward-seeking behavior as a result of the interaction between astrocytes and neurons.

Supplementary Material

Refer to Web version on PubMed Central for supplementary material.

ACKNOWLEDGMENTS AND DISCLOSURES

We thank Dr. Jiang-Fan Chen at Boston University for providing A2AR-Cre mice and Dr. Karl Deisseroth at Stanford University for providing viruses for optogenetics. We thank Anders J. Asp, Dr. Suelen Lucio Boschen De Souza, Seungleal (Brian) Paek, and Dr. J. Luis Lujan at Mayo and Dr. Pat Stemkowski at Inscopix for the helpful comments on the gliotransmitter release and calcium imaging. We thank Dr. Phillip Starski, DeAnn Frederixon for proofreading the paper and helpful comments. This work was supported by the Samuel C. Johnson for Genomics of Addiction Program at Mayo Clinic, the Ulm Foundation, and National Institute on Alcohol Abuse and Alcoholism (K01 AA027773 to SK, R01 AA018779 to DSC). The Mayo Clinic Metabolomics Core was supported by NIH (U24 DK100469).

SK, SIH, DSC conceived and designed all the experiments. SK, SIH, and JYL analyzed the data. SK performed the stereotaxic surgery and *ex vivo* electrophysiology. SIH performed the stereotaxic surgery and animal behavioral evaluation. SK, JYL, SC performed optogenetics and *in vivo* electrophysiology. SK and LP performed microdialysis. SK, HIK, HK performed immunofluorescence. HIK and SC performed western blotting. SK, SIH, MB, DSC wrote the manuscript. All the authors reviewed and confirmed the manuscript.

DSC is a scientific advisory board member to Peptron Inc. and the Peptron had no role in preparation, review, or approval of the manuscript; nor the decision to submit the manuscript for publication. All the other authors declare no biomedical financial interests or potential conflicts of interest.

REFERENCES

1. Yin HH, Knowlton BJ (2006): The role of the basal ganglia in habit formation. Nat Rev Neurosci. 7:464–476. [PubMed: 16715055]
2. Corbit LH, Nie H, Janak PH (2012): Habitual alcohol seeking: time course and the contribution of subregions of the dorsal striatum. Biol Psychiatry. 72:389–395. [PubMed: 22440617]
3. Barker JM, Glen WB, Linsenbardt DN, Lapish CC, Chandler LJ (2017): Habitual Behavior Is Mediated by a Shift in Response-Outcome Encoding by Infralimbic Cortex. eNeuro. 4.
4. Martin R, Bajo-Graneras R, Moratalla R, Perea G, Araque A (2015): Circuit-specific signaling in astrocyte-neuron networks in basal ganglia pathways. Science. 349:730–734. [PubMed: 26273054]
5. Melzer S, Gil M, Koser DE, Michael M, Huang KW, Monyer H (2017): Distinct Corticostriatal GABAergic Neurons Modulate Striatal Output Neurons and Motor Activity. Cell Rep. 19:1045–1055. [PubMed: 28467898]
6. Augustin SM, Chancey JH, Lovinger DM (2018): Dual Dopaminergic Regulation of Corticostriatal Plasticity by Cholinergic Interneurons and Indirect Pathway Medium Spiny Neurons. Cell Rep. 24:2883–2893. [PubMed: 30208314]
7. Johansson Y, Silberberg G (2020): The Functional Organization of Cortical and Thalamic Inputs onto Five Types of Striatal Neurons Is Determined by Source and Target Cell Identities. Cell Rep. 30:1178–1194 e1173. [PubMed: 31995757]
8. Fuxe K, Marcellino D, Genedani S, Agnati L (2007): Adenosine A(2A) receptors, dopamine D(2) receptors and their interactions in Parkinson's disease. Mov Disord. 22:1990–2017. [PubMed: 17618524]
9. Gokce O, Stanley GM, Treutlein B, Neff NF, Camp JG, Malenka RC, et al. (2016): Cellular Taxonomy of the Mouse Striatum as Revealed by Single-Cell RNA-Seq. Cell Rep. 16:1126–1137. [PubMed: 27425622]
10. Martin A, Calvigioni D, Tzortzi O, Fuzik J, Warnberg E, Meletis K (2019): A Spatiomolecular Map of the Striatum. Cell Rep. 29:4320–4333 e4325. [PubMed: 31875543]
11. Balleine BW, Delgado MR, Hikosaka O (2007): The role of the dorsal striatum in reward and decision-making. J Neurosci. 27:8161–8165. [PubMed: 17670959]
12. Gremel CM, Costa RM (2013): Orbitofrontal and striatal circuits dynamically encode the shift between goal-directed and habitual actions. Nat Commun. 4:2264. [PubMed: 23921250]
13. Li Y, Pan X, He Y, Ruan Y, Huang L, Zhou Y, et al. (2018): Pharmacological Blockade of Adenosine A2A but Not A1 Receptors Enhances Goal-Directed Valuation in Satiety-Based Instrumental Behavior. Front Pharmacol. 9:393. [PubMed: 29740319]
14. Li Y, He Y, Chen M, Pu Z, Chen L, Li P, et al. (2016): Optogenetic Activation of Adenosine A2A Receptor Signaling in the Dorsomedial Striatopallidal Neurons Suppresses Goal-Directed Behavior. Neuropsychopharmacology. 41:1003–1013. [PubMed: 26216520]
15. Kim R, Healey KL, Sepulveda-Orengo MT, Reissner KJ (2018): Astroglial correlates of neuropsychiatric disease: From astrocytopathy to astrogliosis. Prog Neuropsychopharmacol Biol Psychiatry. 87:126–146. [PubMed: 28989099]
16. Haydon PG, Nedergaard M (2014): How do astrocytes participate in neural plasticity? Cold Spring Harb Perspect Biol. 7:a020438. [PubMed: 25502516]
17. Adamsky A, Kol A, Kreisel T, Doron A, Ozeri-Engelhard N, Melcer T, et al. (2018): Astrocytic Activation Generates De Novo Neuronal Potentiation and Memory Enhancement. Cell. 174:59–71 e14. [PubMed: 29804835]
18. Chen N, Sugihara H, Kim J, Fu Z, Barak B, Sur M, et al. (2016): Direct modulation of GFAP-expressing glia in the arcuate nucleus bi-directionally regulates feeding. Elife. 5.
19. Araque A, Carmignoto G, Haydon PG, Oliet SH, Robitaille R, Volterra A (2014): Gliotransmitters travel in time and space. Neuron. 81:728–739. [PubMed: 24559669]

20. Perea G, Navarrete M, Araque A (2009): Tripartite synapses: astrocytes process and control synaptic information. Trends Neurosci. 32:421–431. [PubMed: 19615761]
21. Scofield MD, Boger HA, Smith RJ, Li H, Haydon PG, Kalivas PW (2015): Gq-DREADD Selectively Initiates Glial Glutamate Release and Inhibits Cue-induced Cocaine Seeking. Biol Psychiatry. 78:441–451. [PubMed: 25861696]
22. Henneberger C, Papouin T, Oliet SHR, Rusakov DA (2010): Long-term potentiation depends on release of D-serine from astrocytes. Nature. 463:232–U120. [PubMed: 20075918]
23. Perea G, Araque A (2007): Astrocytes potentiate transmitter release at single hippocampal synapses. Science. 317:1083–1086. [PubMed: 17717185]
24. Panatier A, Vallee J, Haber M, Murai KK, Lacaille JC, Robitaille R (2011): Astrocytes are endogenous regulators of basal transmission at central synapses. Cell. 146:785–798. [PubMed: 21855979]
25. Corkrum M, Covelo A, Lines J, Bellocchio L, Pisansky M, Loke K, et al. (2020): Dopamine-Evoked Synaptic Regulation in the Nucleus Accumbens Requires Astrocyte Activity. Neuron. 105:1036–1047 e1035. [PubMed: 31954621]
26. Cui W, Mizukami H, Yanagisawa M, Aida T, Nomura M, Isomura Y, et al. (2014): Glial dysfunction in the mouse habenula causes depressive-like behaviors and sleep disturbance. J Neurosci. 34:16273–16285. [PubMed: 25471567]
27. Choi DS, Cascini MG, Mailliard W, Young H, Paredes P, McMahon T, et al. (2004): The type 1 equilibrative nucleoside transporter regulates ethanol intoxication and preference. Nat Neurosci. 7:855–861. [PubMed: 15258586]
28. Nam HW, Lee MR, Zhu Y, Wu J, Hinton DJ, Choi S, et al. (2011): Type 1 equilibrative nucleoside transporter regulates ethanol drinking through accumbal N-methyl-D-aspartate receptor signaling. Biol Psychiatry. 69:1043–1051. [PubMed: 21489406]
29. Renteria R, Baltz ET, Gremel CM (2018): Chronic alcohol exposure disrupts top-down control over basal ganglia action selection to produce habits. Nat Commun. 9:211. [PubMed: 29335427]
30. Hadjas LC, Luscher C, Simmler LD (2019): Aberrant habit formation in the Sapap3-knockout mouse model of obsessive-compulsive disorder. Sci Rep. 9:12061. [PubMed: 31427755]
31. Calabresi P, Centonze D, Pisani A, Sancesario G, Gubellini P, Marfia GA, et al. (1998): Striatal spiny neurons and cholinergic interneurons express differential ionotropic glutamatergic responses and vulnerability: implications for ischemia and Huntington's disease. Ann Neurol. 43:586–597. [PubMed: 9585352]
32. Tozzi A, de Iure A, Di Filippo M, Tantucci M, Costa C, Borsini F, et al. (2011): The distinct role of medium spiny neurons and cholinergic interneurons in the D(2)/A(2)A receptor interaction in the striatum: implications for Parkinson's disease. J Neurosci. 31:1850–1862. [PubMed: 21289195]
33. Durkee CA, Covelo A, Lines J, Kofuji P, Aguilar J, Araque A (2019): Gi/o protein-coupled receptors inhibit neurons but activate astrocytes and stimulate gliotransmission. Glia. 67:1076–1093. [PubMed: 30801845]
34. Bazargani N, Attwell D (2016): Astrocyte calcium signaling: the third wave. Nat Neurosci. 19:182–189. [PubMed: 26814587]
35. Agulhon C, Boyt KM, Xie AX, Friocourt F, Roth BL, McCarthy KD (2013): Modulation of the autonomic nervous system and behaviour by acute glial cell Gq protein-coupled receptor activation in vivo. J Physiol. 591:5599–5609. [PubMed: 24042499]
36. Chai H, Diaz-Castro B, Shigetomi E, Monte E, Octeau JC, Yu X, et al. (2017): Neural Circuit-Specialized Astrocytes: Transcriptomic, Proteomic, Morphological, and Functional Evidence. Neuron. 95:531–549 e539. [PubMed: 28712653]
37. Bull C, Freitas KC, Zou S, Poland RS, Syed WA, Urban DJ, et al. (2014): Rat nucleus accumbens core astrocytes modulate reward and the motivation to self-administer ethanol after abstinence. Neuropsychopharmacology. 39:2835–2845. [PubMed: 24903651]
38. Martin-Fernandez M, Jamison S, Robin LM, Zhao Z, Martin ED, Aguilar J, et al. (2017): Synapse-specific astrocyte gating of amygdala-related behavior. Nat Neurosci. 20:1540–1548. [PubMed: 28945222]
39. Yang L, Qi Y, Yang Y (2015): Astrocytes control food intake by inhibiting AGRP neuron activity via adenosine A1 receptors. Cell Rep. 11:798–807. [PubMed: 25921535]

40. Reissner KJ, Pletnikov MV (2020): Contributions of nonneuronal brain cells in substance use disorders. Neuropsychopharmacology. 45:224–225. [PubMed: 31477816]
41. Chen TW, Wardill TJ, Sun Y, Pulver SR, Renninger SL, Baohan A, et al. (2013): Ultrasensitive fluorescent proteins for imaging neuronal activity. Nature. 499:295–300. [PubMed: 23868258]
42. Deutch AY, Colbran RJ, Winder DJ (2007): Striatal plasticity and medium spiny neuron dendritic remodeling in parkinsonism. Parkinsonism Relat Disord. 13 Suppl 3:S251–258. [PubMed: 18267246]
43. Valjent E, Bertran-Gonzalez J, Herve D, Fisone G, Girault JA (2009): Looking BAC at striatal signaling: cell-specific analysis in new transgenic mice. Trends Neurosci. 32:538–547. [PubMed: 19765834]
44. Cheng Y, Huang CCY, Ma T, Wei X, Wang X, Lu J, et al. (2017): Distinct Synaptic Strengthening of the Striatal Direct and Indirect Pathways Drives Alcohol Consumption. Biol Psychiatry. 81:918–929. [PubMed: 27470168]
45. Hong SI, Kang S, Chen JF, Choi DS (2019): Indirect Medium Spiny Neurons in the Dorsomedial Striatum Regulate Ethanol-Containing Conditioned Reward Seeking. J Neurosci. 39:7206–7217. [PubMed: 31315945]
46. Nam HW, Hinton DJ, Kang NY, Kim T, Lee MR, Oliveros A, et al. (2013): Adenosine transporter ENT1 regulates the acquisition of goal-directed behavior and ethanol drinking through A2A receptor in the dorsomedial striatum. J Neurosci. 33:4329–4338. [PubMed: 23467349]
47. Macpherson T, Morita M, Hikida T (2014): Striatal direct and indirect pathways control decision-making behavior. Front Psychol. 5:1301. [PubMed: 25429278]
48. Gesiarz F, Crockett MJ (2015): Goal-directed, habitual and Pavlovian prosocial behavior. Front Behav Neurosci. 9:135. [PubMed: 26074797]
49. Halassa MM, Fellin T, Haydon PG (2007): The tripartite synapse: roles for gliotransmission in health and disease. Trends Mol Med. 13:54–63. [PubMed: 17207662]
50. Yu X, Taylor AMW, Nagai J, Golshani P, Evans CJ, Coppola G, et al. (2018): Reducing Astrocyte Calcium Signaling In Vivo Alters Striatal Microcircuits and Causes Repetitive Behavior. Neuron. 99:1170–1187 e1179. [PubMed: 30174118]
51. Savtchouk I, Di Castro MA, Ali R, Stubbe H, Lujan R, Volterra A (2019): Circuit-specific control of the medial entorhinal inputs to the dentate gyrus by atypical presynaptic NMDARs activated by astrocytes. Proc Natl Acad Sci U S A. 116:13602–13610. [PubMed: 31152131]
52. Lalo U, Palygin O, Rasooli-Nejad S, Andrew J, Haydon PG, Pankratov Y (2014): Exocytosis of ATP from astrocytes modulates phasic and tonic inhibition in the neocortex. PLoS Biol. 12:e1001747. [PubMed: 24409095]
53. Deaglio S, Robson SC (2011): Ectonucleotidases as regulators of purinergic signaling in thrombosis, inflammation, and immunity. Adv Pharmacol. 61:301–332. [PubMed: 21586363]
54. Pastor-Anglada M, Perez-Torras S (2018): Who Is Who in Adenosine Transport. Front Pharmacol. 9:627. [PubMed: 29962948]
55. Santello M, Volterra A (2009): Synaptic modulation by astrocytes via Ca2+-dependent glutamate release. Neuroscience. 158:253–259. [PubMed: 18455880]
56. Nam HW, Lee MR, Hinton DJ, Choi DS (2010): Reduced effect of NMDA glutamate receptor antagonist on ethanol-induced ataxia and striatal glutamate levels in mice lacking ENT1. Neurosci Lett. 479:277–281. [PubMed: 20570605]
57. Min R, Nevian T (2012): Astrocyte signaling controls spike timing-dependent depression at neocortical synapses. Nat Neurosci. 15:746–753. [PubMed: 22446881]
58. Martin ED, Fernandez M, Perea G, Pascual O, Haydon PG, Araque A, et al. (2007): Adenosine released by astrocytes contributes to hypoxia-induced modulation of synaptic transmission. Glia. 55:36–45. [PubMed: 17004232]
59. Covelo A, Araque A (2016): Lateral regulation of synaptic transmission by astrocytes. Neuroscience. 323:62–66. [PubMed: 25732135]
60. Fino E, Vandecasteele M, Perez S, Saudou F, Venance L (2018): Region-specific and state-dependent action of striatal GABAergic interneurons. Nat Commun. 9:3339. [PubMed: 30131490]

61. Guo Q, Wang D, He X, Feng Q, Lin R, Xu F, et al. (2015): Whole-brain mapping of inputs to projection neurons and cholinergic interneurons in the dorsal striatum. PLoS One. 10:e0123381. [PubMed: 25830919]

62. Corkrum M, Rothwell PE, Thomas MJ, Kofuji P, Araque A (2019): Opioid-Mediated Astrocyte-Neuron Signaling in the Nucleus Accumbens. Cells. 8.

63. Casper KB, McCarthy KD (2006): GFAP-positive progenitor cells produce neurons and oligodendrocytes throughout the CNS. Mol Cell Neurosci. 31:676–684. [PubMed: 16458536]

64. Khakh BS (2019): Astrocyte-Neuron Interactions in the Striatum: Insights on Identity, Form, and Function. Trends Neurosci. 42:617–630. [PubMed: 31351745]

65. Hilario MR, Costa RM (2008): High on habits. Front Neurosci. 2:208–217. [PubMed: 19225594]

66. Lee JH, Kwon H, Choi J, Yang BH (2007): Cue-exposure therapy to decrease alcohol craving in virtual environment. Cyberpsychol Behav. 10:617–623. [PubMed: 17927528]

67. Gomez JL, Bonaventura J, Lesniak W, Mathews WB, Sysa-Shah P, Rodriguez LA, et al. (2017): Chemogenetics revealed: DREADD occupancy and activation via converted clozapine. Science. 357:503–507. [PubMed: 28774929]

68. Jendryka M, Palchaudhuri M, Ursu D, van der Veen B, Liss B, Katzel D, et al. (2019): Pharmacokinetic and pharmacodynamic actions of clozapine-N-oxide, clozapine, and compound 21 in DREADD-based chemogenetics in mice. Sci Rep. 9:4522. [PubMed: 30872749]

69. Runegaard AH, Fitzpatrick CM, Woldbye DPD, Andreasen JT, Sorensen AT, Gether U (2019): Modulating Dopamine Signaling and Behavior with Chemogenetics: Concepts, Progress, and Challenges. Pharmacol Rev. 71:123–156. [PubMed: 30814274]

70. Thompson KJ, Khajehali E, Bradley SJ, Navarrete JS, Huang XP, Slocum S, et al. (2018): DREADD Agonist 21 Is an Effective Agonist for Muscarinic-Based DREADDs in Vitro and in Vivo. ACS Pharmacol Transl Sci. 1:61–72. [PubMed: 30868140]

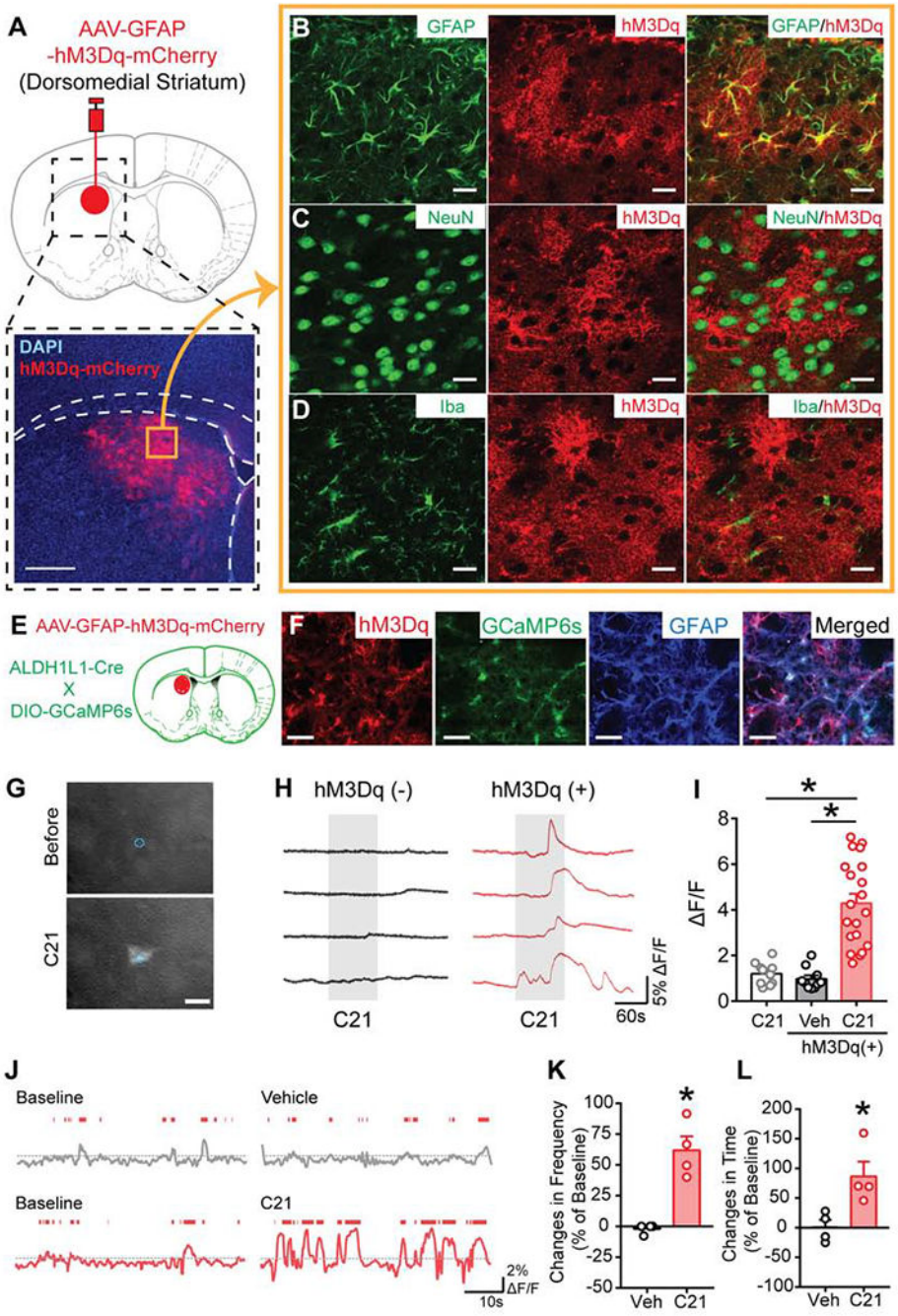

Figure 1.

The selective expression and activation of DREADDs induce calcium signaling in the astrocytes of the DMS. **(A)** A representative image of GFAP promoter-driven hM3Dq-mCherry expression in the dorsomedial striatum (DMS). Scale bar = 500 μm. **(B-D)** Immunostaining of GFAP (B), NeuN (C), Iba (D) in the DMS after the GFAP promoter-driven expression of hM3Dq-mCherry. Scale bar = 20 μm. **(E)** Experimental scheme explaining injection of GFAP-promoter driven hM3Dq expressing virus in the DMS of the mice expressing GCaMP6s in the ALDH1L1 positive cells. **(F)** A representative image of

expression of hM3Dq-mCherry in the DMS of Aldh1L1-specific GCaMP6s-expressing mice. Scale bar = 50 μm. **(G-I)** The representative figure (G), traces (H) and pooled data (I) showing that bath application of compound 21 (C21, 10 μM) increases the intracellular Ca^{2+} in the astrocyte of DMS. One-way ANOVA followed by Tukey's multiple comparisons test. N_{cell} = 10 (2 mice)/group (C21 without hM3Dq and Veh with hM3Dq) and 20 (3 mice, C21 with hM3Dq). Data represented as mean ± SEM. *P<0.05. Scale bar = 10 μm. **(J-L)** The representative traces (J) and pooled data (K-L) showing that systemic administration of C21 (1 mg/kg, *i.p.*) increase the intracellular Ca^{2+} in the astrocytes in the DMS of freely moving mice. N_{mice} = 4/group. Data represented as mean ± SEM. paired *t*-test, *P<0.05.

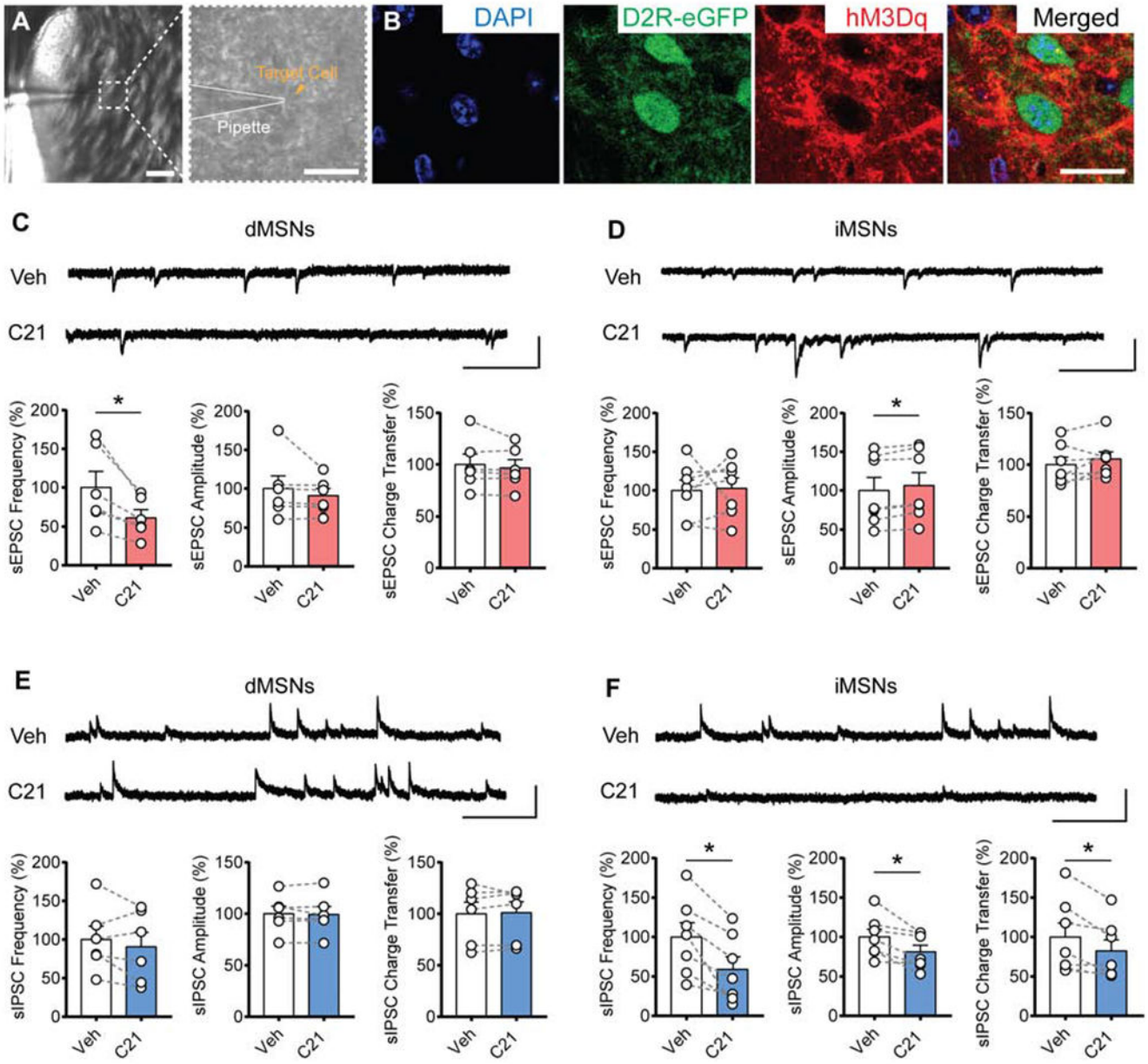

Figure 2.

Chemogenetic activation of the DMS astrocytes regulates the synaptic events in the direct and indirect MSNs differently. **(A,B)** CCD camera (A) and confocal (B) captured images showing the condition of recordings in the DMS indirect medium spiny neurons (iMSNs). Scale bars = 250 μm (A left), 50 μm (A right), and 20 μm (B). **(C-F)** The effects of bath application of C21 (10 μM) on the spontaneous excitatory postsynaptic currents (sEPSCs, C, D, Scale bars = 250 ms, 20 pA) and inhibitory postsynaptic currents (sIPSCs, E, F, Scale bars = 500 ms, 30 pA) in the dMSNs and the iMSNs. dMSNs sEPSCs: N_{cell} = 6 (3 mice), iMSNs sEPSCs: N_{cell} = 7 (4 mice), dMSNs sIPSCs: N_{cell} = 6 (3 mice), iMSNs sIPSCs: N_{cell} = 7 (3 mice). Data represented as mean ± SEM. paired *t*-test, *P<0.05.

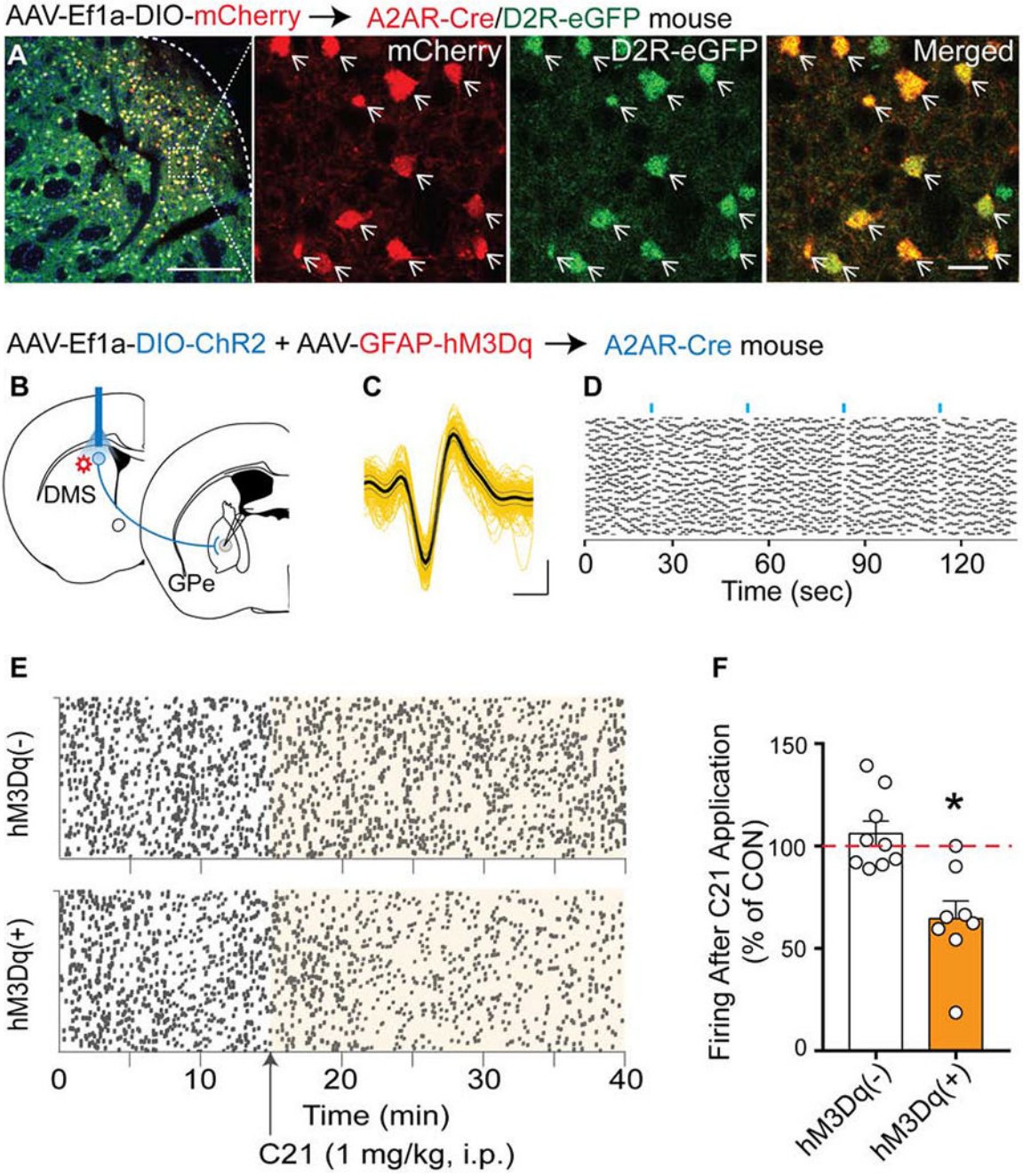

Figure 3.

Local activation of the DMS astrocytes regulates the neuronal activities in the downstream of the DMS. **(A)** The representative figure showing the co-localization of D2R and A2AR in the DMS. Scale bars = 100 μm (Left) and 20 μm (Right). **(B)** Experimental scheme. **(C,D)** Traces of GPe spontaneous firing that is inhibited by light stimulation of the iMSNs in the DMS. Scale bar = 0.3 ms, 200 μV. **(E, F)** The representative figure (E) and pooled data (F) showing the firing rate of the GPe neurons before and after systemic administration of C21

(1 mg/kg, *i.p.*). N_{mice} = 8-9/group. Data represented as mean ± SEM. unpaired *t*-test, *P<0.05.

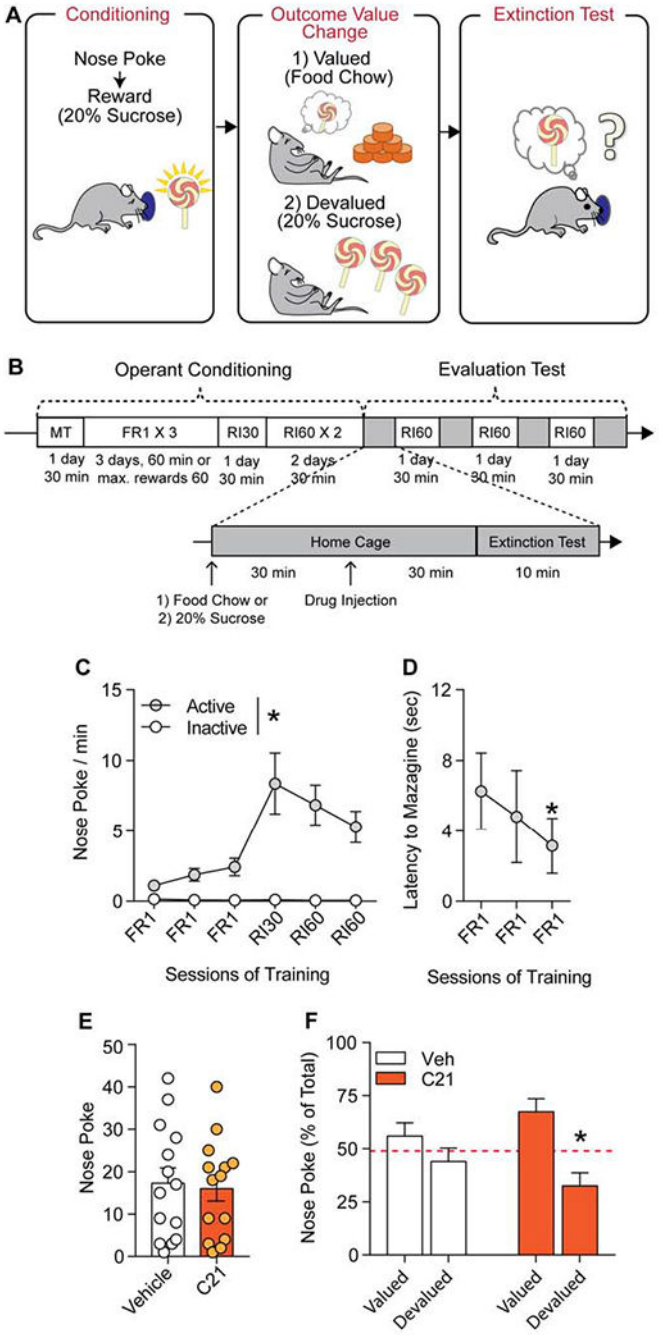

Figure 4.

Astrocytic activation shifts the reward-seeking patterns from habitual action to goal-directed behaviors. **(A,B)** Experimental scheme. **(C,D)** Nose-poking behavior (C) and Latency to Magazine (D) during operant conditioning. two-way ANOVA followed by Tukey's multiple comparisons test. Data represented as mean ± SEM. *P<0.05. **(E)** The total amount of nose-poking in the valued state. Data represented as mean ± SEM. paired *t*-test, P>0.05. **(F)** Comparison of nose-poking changes between the valued (chow) and the devalued (20%

sucrose) states after the application of Vehicle or C21 (*i.p.*, 1 mg/kg). N_{mice} = 14/group. Data represented as mean ± SEM. paired *t*-test, *P<0.05.

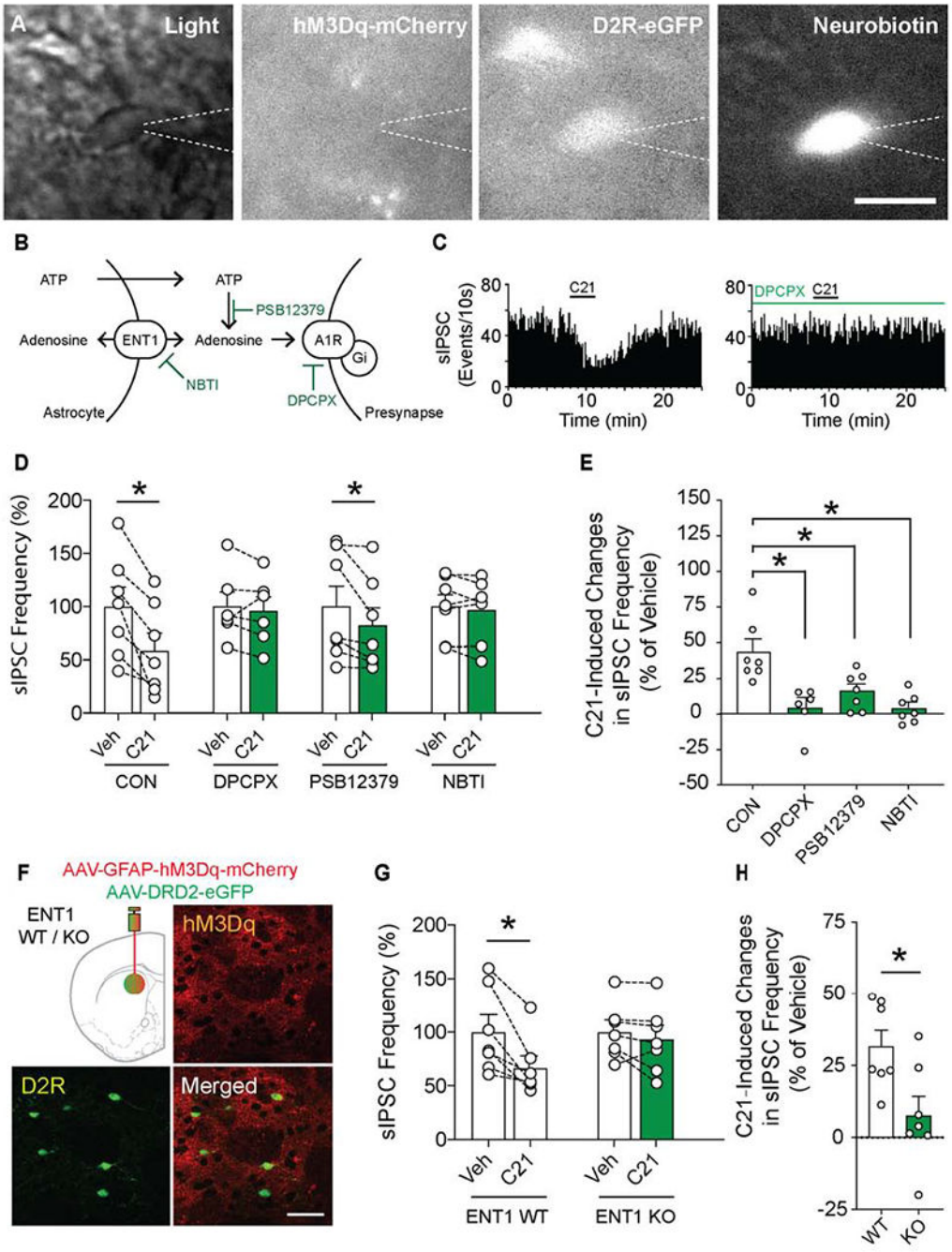

Figure 5.

Adenosinergic signaling is involved in the astrocytic activation-induced adaptation of the DMS neurons and behaviors. **(A)** CCD camera and fluorescence-filtered images showing the recorded DMS indirect medium spiny neurons (iMSNs). Scale bar = 20 μm. **(B)** Experimental Scheme. **(C)** The representative traces showing the effects of bath application of C21 (10 μM) on the spontaneous inhibitory postsynaptic currents (sIPSCs) in the iMSNs with or without pretreatment of DPCPX (A1R antagonist, 1 μM). **(D)** Pooled data showing the effects of the pretreatment of DPCPX [1 μM, N_{cell} = 6 (3 mice)], PSB12379 [CD73

inhibitor, 10 μM, N_{cell} = 7 (4 mice)], and NBTI [ENT1 inhibitor, 10 μM, N_{cell} = 7 (3 mice)] on the frequency of sIPSCs in the iMSNs of the DMS. Data represented as mean ± SEM. Paired *t*-test, *P<0.05. **(E)** The comparison of the C21-induced changes in the sIPSCs in the iMSNs of the DMS by the drug pretreatment with CON. N_{cell} = 6-7 (3-4 mice)/group. Data represented as mean ± SEM. one-way ANOVA followed by Tukey's multiple comparisons test. *P<0.05. **(F)** A representative image of GFAP promoter-driven hM3Dq-mCherry and DRD2 promoter-driven eGFP expression in the dorsomedial striatum (DMS) of ENT1 transgenic mouse. Scale bar = 50 μm. **(G)** Pooled data showing the effects of the C21 application on the sIPSCs in the iMSNs of ENT1 WT and KO mice. N_{cell} = 7 (3 mice)/ group. Data represented as mean ± SEM. Paired *t*-test, *P<0.05. (H) The comparison of the changes in the sIPSCs. N_{cell} = 7 (3 mice)/group. Data represented as mean ± SEM. Unpaired *t*-test, *P<0.05.

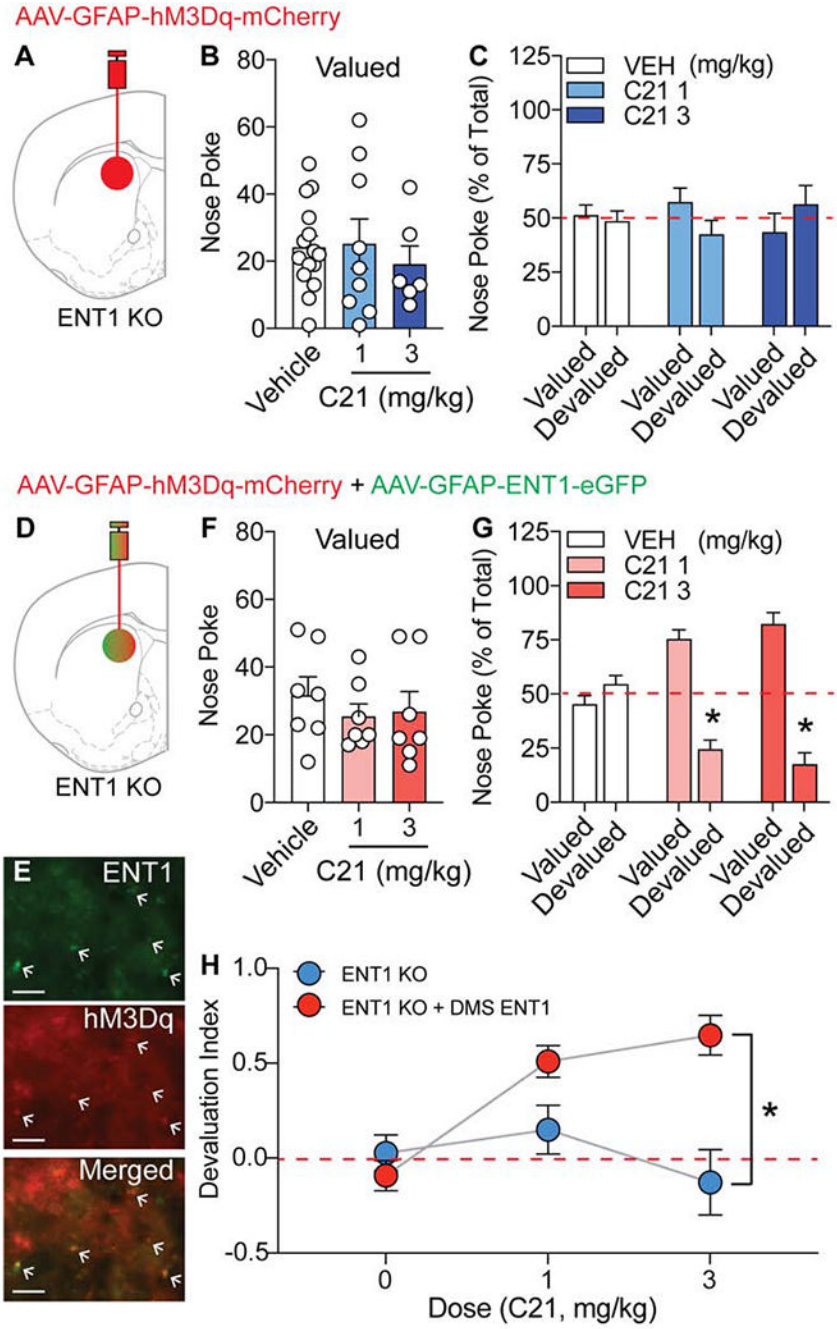

Figure 6.

DMS ENT1 rescue in ENT1 KO mice can restore the behavioral shift in the reward-seeking induced by astrocytic activation. **(A)** Experimental scheme explaining injection of GFAP-promoter driven hM3Dq expressing virus in the DMS of ENT1 KO mice. **(B)** The total amount of nose-poking in the valued state. One-way ANOVA followed by Tukey's multiple comparisons test, NS. **(C)** Comparison of nose-poking changes between the valued (chow) and the devalued (20% sucrose) states after application of Vehicle or C21 (*i.p.*, 1 and 3 mg/kg) in the ENT1 KO mice. N_{mice} = 6-15/group. Data represented as mean ± SEM. Paired

t-test, NS. **(D,E)** Experimental scheme (D) and representative image (E) showing injection of GFAP promoter-driven hM3Dq and mENT1 expressing viruses in the DMS of ENT1 KO mice. Scale bar = 40 μm. **(F)** The total amount of nose-poking in the valued state. One-way ANOVA followed by Tukey's multiple comparisons test, NS. **(G)** Comparison of nose-poking changes between the valued (chow) and the devalued (20% sucrose) states after application of Vehicle or C21 (*i.p.*, 1 and 3 mg/kg) in the ENT1 rescued mice. N_{mice} = 7/group. Data represented as mean ± SEM. Paired *t*-test. *P<0.05. **(H)** Devaluation Index showing the differences between ENT1 KO and ENT1 rescued mice. N_{mice} = 6-15/group. Data represented as mean ± SEM. two-way ANOVA followed by Tukey's multiple comparisons test. *P<0.05.

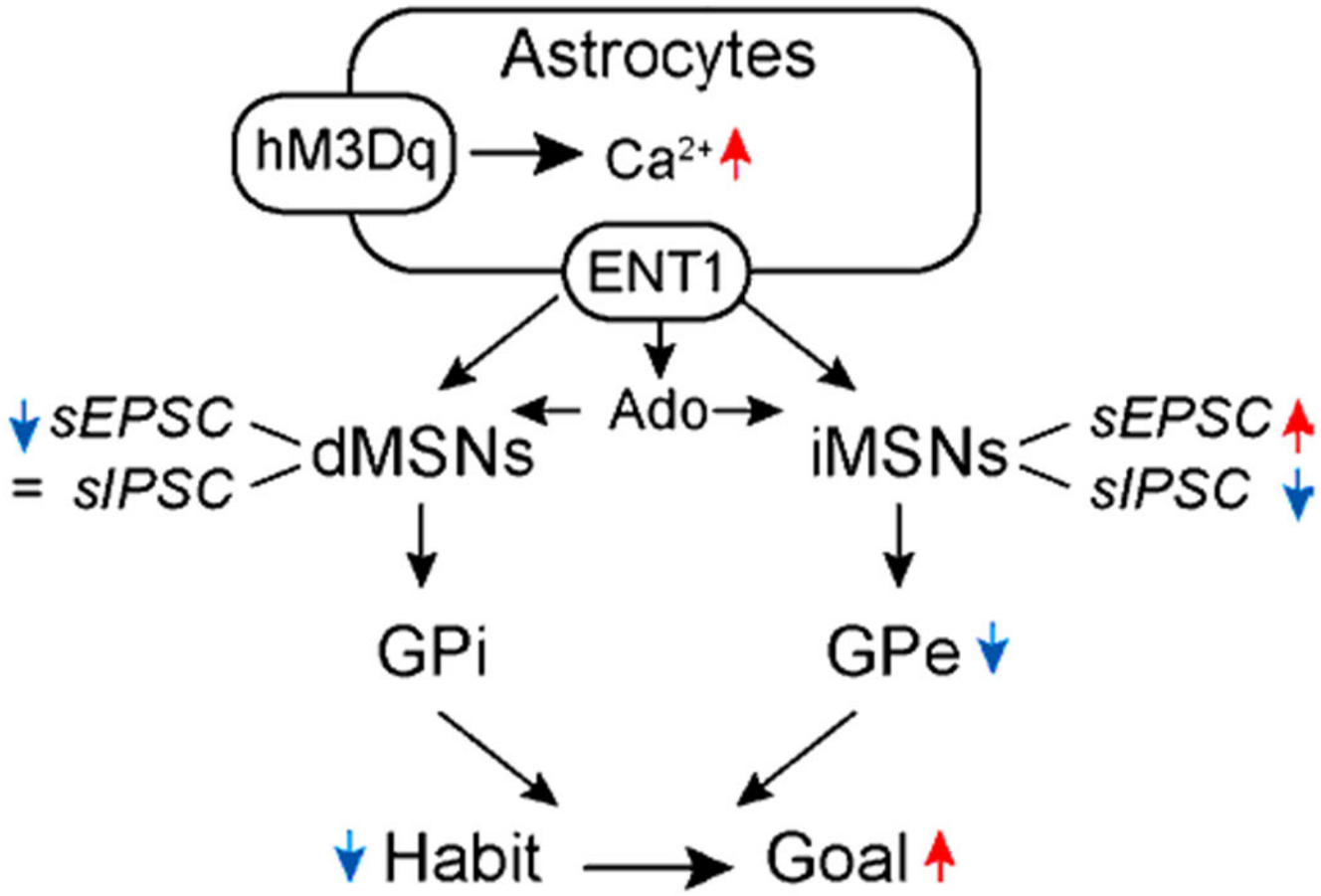

Figure 7.

The chemogenetic activation of astrocytes in the dorsomedial striatum modulates the synaptic activities of direct and indirect medium spiny neurons (dMSNs and iMSNs) differentially and those of downstream via adenosine signaling, which leads to a transition to goal-directed reward-seeking behavior. hM3Dq, modified form of the human M3 muscarinic (hM3) receptor; ENT1, equlibrative nucleoside transporter type 1; Ado, adenosine; sEPSCs, synaptic excitatory post-synaptic currents; sIPSCs, synaptic inhibitory post-synaptic currents; GPi, internal globus pallidus; GPe, external globus pallidus.

KEY RESOURCES TABLE

Resource Type	Specific Reagent or Resource	Source or Reference	Identifiers	Additional Information
Add additional rows as needed for each resource type	Include species and sex when applicable.	Include name of manufacturer, company, repository, individual, or research lab. Include PMID or DOI for references; use “this paper” if new.	Include catalog numbers, stock numbers, database IDs or accession numbers, and/or RRIDs. RRIDs are highly encouraged; search for RRIDs at https://scicrunch.org/resources.	Include any additional information or notes if necessary.
Antibody	GFAP, mouse monoclonal	EMD Millipore	MAB360	1:500
Antibody	NeuN, mouse monoclonal	Abcam	Ab104224	1:1000
Antibody	Iba, rabbit monoclonal	Abcam	Ab178847	1:500
Antibody	A1R, rabbit polyclonal	Alomone Labs	AAR-006	1:500
Antibody	A2R, rabbit polyclonal	Alomone Labs	AAR-002	1:500
Antibody	GAPDH, mouse monoclonal	EMD Millopore	MAB374	1:2000
Bacterial or Viral Strain	AAV5-GFAP-hM3Dq-mCherry	University of North Carolina Vector Core	N/A	N/A
Bacterial or Viral Strain	AAV5-EF1α-DIO-hChR2-eYFP	Add gene	#20298	N/A
Bacterial or Viral Strain	AAV9-DRD2-eGFP, AAV5-GFAP-mENT1-eGFP, AAV5-GFAP-mENT1-mCherry	Vector Biolab	N/A	N/A
Chemical Compound or Drug	DPCPX	Tocris	#0439	N/A
Chemical Compound or Drug	PSB12379	Tocris	#6083	N/A
Chemical Compound or Drug	NBTI (NBMPR)	Tocris	#2924	N/A
Chemical Compound or Drug	DNQX	Tocris	#2312	N/A
Chemical Compound or Drug	AP5	Tocris	#3693	N/A
Chemical Compound or Drug	Picrotoxin	Tocris	#1128	N/A
Chemical Compound or Drug	Compound 21	Hello Bio	HB6124	N/A
Genetic Reagent	Mouse, Adora2A-Cre	Dr. Jiang-Fan Chen at Wenzhou Medical University	MMRRC: 031168-UCD	N/A
Genetic Reagent	Mouse, ALDH1L1-Cre	Jackson Laboratory	#23748	N/A
Genetic Reagent	Mouse, DrD2-eGFP	Jackson Laboratory	#030255	N/A
Genetic Reagent	Mouse, DRD1-tdTomato	Jackson Laboratory	#016204	N/A
Genetic Reagent	Mouse, ENT1 KO	PMID: 15258586	N/A	N/A
Organism/Strain	Mouse, C57BL/6J	Jackson Laboratory	N/A	N/A
Software; Algorithm	MATLAB R2019a (v9.6)	Mathworks	RRID:SCR_001622	N/A